Title

RNA polymerase II-driven CRISPR-Cas9 system for efficient non-growth-biased metabolic engineering of Kluyveromyces marxianus.

Authors

Bever, Danielle
Wheeldon, Ian
Da Silva, Nancy

Publication Date

2022-12-01

DOI

10.1016/j.mec.2022.e00208

Peer reviewed

Metabolic Engineering Communications 15 (2022) e00208

Contents lists available at ScienceDirect

Metabolic Engineering Communications

journal homepage: www.elsevier.com/locate/mec

RNA polymerase II-driven CRISPR-Cas9 system for efficient non-growth-biased metabolic engineering of *Kluyveromyces marxianus*

Danielle Bever [a], Ian Wheeldon [b], Nancy Da Silva [a,*]

[a] Department of Chemical and Biomolecular Engineering, University of California, Irvine, CA, 92697, USA
[b] Department of Chemical and Environmental Engineering, University of California, Riverside, CA, 92521, USA

ARTICLE INFO

Keywords:
Kluyveromyces marxianus
CRISPR-Cas9
Polyketides
Metabolic engineering
Thermotolerant yeast

ABSTRACT

The thermotolerant yeast *Kluyveromyces marxianus* has gained significant attention in recent years as a promising microbial candidate for industrial biomanufacturing. Despite several contributions to the expanding molecular toolbox for gene expression and metabolic engineering of *K. marxianus*, there remains a need for a more efficient and versatile genome editing platform. To address this, we developed a CRISPR-based editing system that enables high efficiency marker-less gene disruptions and integrations using only 40 bp homology arms in NHEJ functional and non-functional *K. marxianus* strains. The use of a strong RNA polymerase II promoter allows efficient expression of gRNAs flanked by the self-cleaving RNA structures, tRNA and HDV ribozyme, from a single plasmid co-expressing a codon optimized Cas9. Implementing this system resulted in nearly 100% efficiency of gene disruptions in both NHEJ-functional and NHEJ-deficient *K. marxianus* strains, with donor integration efficiencies reaching 50% and 100% in the two strains, respectively. The high gRNA targeting performance also proved instrumental for selection of engineered strains with lower growth rate but improved polyketide biosynthesis by avoiding an extended outgrowth period, a common method used to enrich for edited cells but that fails to recover advantageous mutants with even slightly impaired fitness. Finally, we provide the first demonstration of simultaneous, markerless integrations at multiple loci in *K. marxianus* using a 2.6 kb and a 7.6 kb donor, achieving a dual integration efficiency of 25.5% in a NHEJ-deficient strain. These results highlight both the ease of use and general robustness of this system for rapid and flexible metabolic engineering in this non-conventional yeast.

1. Introduction

The recent advent of sophisticated sequencing and CRISPR-Cas9 technologies has enabled the engineering of a wide range of non-conventional microorganisms with diverse metabolisms and growth characteristics. *Kluyveromyces marxianus* is a non-conventional yeast that has quickly emerged as a robust heterologous host with excellent characteristics for industrial applications. *K. marxianus* is the fastest growing eukaryote with a doubling time as low as 45 min (Groeneveld et al., 2009). This species grows on a variety of carbon sources including pentose sugars and disaccharides (McTaggart et al., 2019; Nonklang et al., 2008; Urit et al., 2012), is thermotolerant up to 52 °C (Banat et al., 1992) and acid-tolerant to pH 2.3 (Amrane and Prigent, 1998), and has Generally Regarded as Safe (GRAS) and Qualified Presumption of Safety (QPS) status in the United States and European Union, respectively (Lane and Morrissey, 2010). Classified as a Crabtree-negative yeast, *K. marxianus* has also been shown to minimally accumulate common metabolic byproducts such as ethanol, glycerol, and organic acids (Fonseca et al., 2007, 2013), supporting enhanced product yield and separation. These numerous advantageous characteristics have driven the study and successful use of *K. marxianus* for the high-level production of a variety of native and non-native products including ethanol (Charoensopharat et al., 2015; Leonel et al., 2021), 2-phenylethanol (Hillman et al., 2021; Martínez et al., 2018), D-allulose (Yang et al., 2018), and triacetic acid lactone (Lang et al., 2020; McTaggart et al., 2019) from substrates other than purified glucose.

Recent contributions to the toolbox of genetic parts for tunable gene expression in *K. marxianus* include the characterization of native and non-native promoters, terminators, selection markers, and low- and high-copy origins of replication (Kumar et al., 2021; Lang et al., 2020; McTaggart et al., 2019; Rajkumar et al., 2019; Yang et al., 2015). In addition, CRISPR-Cas9 systems have been published by five groups and

* Corresponding author.
E-mail address: ndasilva@uci.edu (N. Da Silva).

https://doi.org/10.1016/j.mec.2022.e00208
Received 16 June 2022; Received in revised form 7 September 2022; Accepted 23 September 2022
Available online 24 September 2022

successfully applied for the synthesis of several compounds, including fatty acids (Cernak et al., 2018), 2-phenylethanol (Li et al., 2021; Rajkumar and Morrissey, 2020), ethyl acetate (Löbs et al., 2017, 2018), human N-glycan structures (Lee et al., 2020), and a single-chain antibody (Nambu-Nishida et al., 2018). A detailed summary of the current *K. marxianus* CRISPR systems can be found in Table S1. Despite the proven utility of these systems, suboptimal features include donors with long homologies (several hundreds of base pairs), donors with selection markers, a growth-biasing selection process, multiple gRNAs to target the same loci, or a high DNA input. A platform with higher efficiency and greater ease of use is thus needed for more robust metabolic engineering of *K. marxianus*. In the design of our system, we aimed for (1) high rates of gene knockout (KO) and gene integration using short 40 base pair (bp) homology arms and modest DNA input during transformation, (2) marker-less integrations, (3) elimination of growth bias by avoiding an extended outgrowth period, (4) reasonably efficient integrations even in a non-homologous end joining (NHEJ)-functional strain, and (5) simultaneous gene integrations at more than one locus.

Most established CRISPR-Cas9 systems in *K. marxianus* use RNA polymerase (RNAP) III promoters for gRNA expression (Cernak et al., 2018; Lee et al., 2018, 2020; Löbs et al., 2017; Nambu-Nishida et al., 2017) to obtain RNA transcripts with minimal end modifications (Marck et al., 2006), a favorable quality to ensure high activity of gRNA. However, a catalog of well-characterized RNAP III promoters does not exist (Gao and Zhao, 2014; Ma et al., 2014) and the rate of RNA expression from such promoters is typically low (Ryan et al., 2014; Turowski and Tollervey, 2016). With weak gRNA expression, many generations are generally required to accumulate sufficient gRNA for efficient complexing with Cas9 and for subsequent genome editing (Ng and Dean, 2017). RNAP II promoters are better characterized and tend to offer higher expression rates (Gao and Zhao, 2014; Ng and Dean, 2017); however, the 5′ cap and 3′ polyA tail end modifications produced by these promoters can hinder gRNA function (Gao and Zhao, 2014; Ng and Dean, 2017). Studies in various yeasts have limited the effects of these end modifications by flanking the gRNA with cleavable RNA structures, such as ribozymes and tRNAs, that remove the transcript end modifications after self-cleavage or RNase activity, respectively, leaving behind the desired, mature gRNA (Gao and Zhao, 2014; Gorter de Vries et al., 2017; Ng and Dean, 2017). It has also been suggested that the addition of these transient structures at the ends of the pre-gRNA may provide protection from degradation by exonucleases (Ng and Dean, 2017; Ryan and Cate, 2014). The hammerhead (HH) and hepatitis delta virus (HDV) ribozymes are common choices for these constructs as self-cleavage does not leave behind extraneous nucleotides (Ke et al., 2007; Pley et al., 1994). However, achieving this clean self-cleavage for the HH ribozyme requires that its 5' end matches the first six nucleotides of the gRNA targeting sequence, complicating cloning processes (Gao and Zhao, 2014; Juergens et al., 2018). It has also been suggested that self-cleaving activity of the HH ribozyme may be a limiting factor to gRNA function. In contrast, utilization of the HDV ribozyme and tRNAs may offer higher efficiency maturation of gRNAs (Ng and Dean, 2017).

To achieve our goals, we developed a streamlined and highly efficient single plasmid CRISPR system that expresses codon-optimized *Cas9* (Löbs et al., 2017) and a gRNA cassette comprised of the strong *S. cerevisiae TDH3* RNAP II promoter to express a tRNA-gRNA-HDV ribozyme gene (TGR). We first evaluated the efficiency of the system for gene KO and gene integration (up to a 7.6 kb insert) in wild-type and non-homologous end joining (NHEJ)-deficient *K. marxianus* strains. We show that high engineering efficiencies can be achieved by this RNAP II TGR system without the use of growth-biasing outgrowth methods. As a demonstration of the utility of this system for metabolic engineering, we knocked out *GPD1 and ZWF1*, fitness-impairing modifications, and integrated the large *ACC1* gene in *K. marxianus* strain CBS 712 to elevate biosynthesis of the polyketide triacetic acid lactone. Finally, leveraging the high efficiency and multiplexing-compatible gRNA expression cassette design, we demonstrated, for the first time, simultaneous, markerless integrations at more than one loci in *K. marxianus.*

Table 1
List of strains and plasmids.

Strain	Features	Source
CBS 712Δ*U*	Δ*URA3*	McTaggart et al. (2019)
CBS 712Δ*U*Δ*K*	Δ*URA3*Δ*KU70*	This work
CBS 712Δ*U-ACC1*	*HIS3::ACC1*	This work
CBS 712Δ*U*Δ*K-ACC1*	Δ*URA3*Δ*KU70 HIS3::ACC1*	This work
CBS 712Δ*U*Δ*K* Δ*ZWF1*	Δ*URA3*Δ*KU70*Δ*ZWF1*	This work
CBS 712Δ*U*Δ*K* Δ*GPD1*	Δ*URA3*Δ*KU70*Δ*GPD1*	This work
Plasmid Name	**Features**	**Source**
KU70-URAblaster	5′ $KU70_{Km}$ (432 bp)-*UB*-3′ $KU70_{Km}$ (440 bp)	Mctaggart (2020)
KU70-UBV2	5′ $KU70_{Km}$ (763 bp)-*UB*-3′ $KU70_{Km}$ (777 bp)	This work
pIW601	$RPR1p_{Km}$-$tRNA_{glyKm}$-*tracrRNA-SUP4t*; $TEF1p_{Sc}$-$Cas9_{Km*}$; CEN/ARS_{Km}	Löbs et al. (2017)
pYTK009	$TDH3p_{Sc}$ part plasmid	Lee et al. (2015)
pYTK050	sgRNA dropout part plasmid	Lee et al. (2015)
pDBtgr-Cas9	$TDH3p_{Sc}$-$tRNA_{glyKm}$-*tracrRNA-HDV-CYC1*t_{Sc}; $TEF1p_{Sc}$-$Cas9_{Km*}$; CEN/ARS_{Km}	This work
pDBtgr-Cas9-HIS3	$TDH3p_{Sc}$-$tRNA_{glyKm}$-*HIS3 gRNA-tracrRNA-HDV-CYC1*t_{Sc}; $TEF1p_{Sc}$-$Cas9_{Km*}$; CEN/ARS_{Km}	This work
pDBtgr-Cas9-LEU2	$TDH3p_{Sc}$-$tRNA_{glyKm}$-*LEU2 gRNA-tracrRNA-HDV-CYC1*t_{Sc}; $TEF1p_{Sc}$-$Cas9_{Km*}$; CEN/ARS_{Km}	This work
RNAP III TG-HIS3	pIW601 with *HIS3 gRNA* and modified tracrRNA	This work
RNAP III TGR	$RPR1p_{Km}$-$tRNA_{glyKm}$-*tracrRNA-HDV-SUP4t*; $TEF1p_{Sc}$-$Cas9_{Km*}$; CEN/ARS_{Km}	This work
RNAP III TGR-HIS3	$RPR1p_{Km}$-$tRNA_{glyKm}$-*HIS3 gRNA-tracrRNA-HDV-SUP4t*; $TEF1p_{Sc}$-$Cas9_{Km*}$; CEN/ARS_{Km}	This work
pDBtDgr-Cas9	$TDH3p_{Sc}$-$tRNA_{glyKm}$-*tracrRNA-HDV*-linker-$tRNA_{glyKm}$-*tracrRNA-HDV-CYC1*t_{Sc}; $TEF1p_{Sc}$-$Cas9_{Km*}$; CEN/ARS_{Km}	This work
pDBtDgr-Cas9-HIS3-LEU2	$TDH3p_{Sc}$-$tRNA_{glyKm}$-*HIS3 gRNA-tracrRNA-HDV*-linker-$tRNA_{glyKm}$-*LEU2 gRNA-tracrRNA-HDV-CYC1*t_{Sc}; $TEF1p_{Sc}$-$Cas9_{Km*}$; CEN/ARS_{Km}	This work
pDBtgr-Cas9-ZWFI	$TDH3p_{Sc}$-$tRNA_{glyKm}$-*ZWFI gRNA-tracrRNA-HDV-CYC1*t_{Sc}; $TEF1p_{Sc}$-$Cas9_{Km*}$; CEN/ARS_{Km}	This work
pDBtgr-Cas9-GPD1	$TDH3p_{Sc}$-$tRNA_{glyKm}$-*GPD1 gRNA-tracrRNA-HDV-CYC1*t_{Sc}; $TEF1p_{Sc}$-$Cas9_{Km*}$; CEN/ARS_{Km}	This work
pCA-A	$ADH2p_{Sc}$-*CYCIt*$_{Sc}$; CEN/ARS_{Km}	McTaggart et al. (2019)
pCA-A-ACC1	$ADH2p_{Sc}$-$ACC1_{Km}$-*CYCIt*$_{Sc}$; CEN/ARS_{Km}	This work
pKD-P2PS	$PGKIp_{Km}$-*2PSHT-CYC1*t_{Sc}; pKDI$_{Kl}$	McTaggart et al. (2019)

2. Materials and methods

2.1. Strains and media

Escherichia coli strain DH5α (Invitrogen, Carlsbad, CA) was used for plasmid maintenance and amplification. *E. coli* cultures were conducted in Luria-Bertani (LB) media supplemented with 150 mg/L ampicillin. *K. marxianus* strain CBS 712 (ATCC, 200963; ATCC®, Manassas, VA) was previously modified for uracil auxotrophy by McTaggart et al. (2019) resulting in base strain CBS 712Δ*U*. *K. marxianus* strains were cultivated in complex YPD medium (10 g/L Bacto yeast extract, 20 g/L Bacto peptone, and 20 g/L dextrose) or selective SC medium (1.7 g/L Bacto yeast nitrogen base without ammonium sulfate, 5 g/L ammonium sulfate, 5 g/L casamino acids, and 50 mg/L adenine) supplemented with various carbon sources: SDCA (20 g/L dextrose), SXCA (10 g/L xylose), or SLCA (9.5 g/L lactose). SXCA and SLCA have equimolar concentrations of carbon. All strains utilized in this study can be found in Table 1.

2.2. CRISPR plasmid construction and donor DNA synthesis

All plasmids and primers used in this work are listed in Tables 1 and S2, respectively. Primers were purchased from IDT DNA (San Diego, CA) as single stranded DNA oligonucleotides. All PCR reactions for cloning and donor DNA synthesis used Q5 High-Fidelity DNA Polymerase (New England BioLabs, Ipswich, MA). Restriction enzymes and NEBuilder HiFi DNA Assembly Master Mix were purchased from New England BioLabs. Sanger sequencing services by Genewiz (Azenta Life Sciences; La Jolla, CA) were utilized to confirm all DNA sequences amplified by PCR for cloning.

To create the RNAP II-driven gRNA expression cassette, five parts were used: (i) the *S. cerevisiae TDH3* promoter isolated from pYTK009 (Lee et al., 2015) using primers pIW601_5′ScTDH3p and 5′KmtRNAgly_3′ScTDH3p; (ii) the *K. marxianus* $tRNA_{gly}$ isolated from pIW601 (Löbs et al., 2017) using primers 5′KmtRNAgly and 3′KmtRNAgly; (iii) the scaffold tracrRNA isolated from pYTK050 (Lee et al., 2015) using primers 3′KmtRNAgly_NheI_5′scaff and 5′HDV_3′scaff; (iv) 60 of the 68 base pairs constituting the hepatitis delta virus (HDV) ribozyme sequence (Gao and Zhao, 2014; Gorter de Vries et al., 2017) ordered as a single stranded oligo, HDV oligo; and (v) the *S. cerevisiae CYC1* terminator isolated from pCA-A (McTaggart et al., 2019) using primers 3′HDV_AvrII_5′ScCYC1t and 3′ScCYC1t_loxP. A series of splicing by overlap extension PCRs combined these five parts into a single fragment. This RNAP II-driven gRNA expression cassette was then cloned into pIW601 digested with AvrII and SacII using NEBuilder HiFi DNA Assembly, replacing the original RNAP III-driven gRNA expression cassette, and completing construction of plasmid pDBtgr-Cas9.

gRNA targeting sequences were selected based on high On-Target Score (Doench et al., 2016) determined by the Benchling (2021) CRISPR tool, and were analyzed by BLAST (Altschul et al., 1990) to ensure a lack of sequence similarity between the last 12 nucleotides of the targeting sequence and the PAM sequence with the rest of the *K. marxianus* genome. To create a modified version of the gRNA expression cassette containing a new 20 base pair targeting sequence, PCR of pDBtgr-Cas9 was conducted using an oligo consisting of the last 18 base pairs of the *K. marxianus* $tRNA_{gly}$, the 20 base pair targeting sequence, followed by the first 20 base pairs of the scaffold tracrRNA (5′ CGAATCCCGTCAGTGTCA$(N)_{20}$GTTTTAGAGCTAGAAATAGC) and the universal tgr insert R primer. This PCR product and pDBtgr-Cas9, previously digested with NheI and AvrII, were then cloned together using NEBuilder HiFi DNA Assembly.

For construction of the double gRNA (dgRNA)-expressing plasmid, an additional TGR repeat was synthesized through two PCRs of the original TGR cassette using primers that resulted in addition of a linker sequence between the TGR tandem repeats as in Gorter de Vries et al. (2017) using primers 3′HDV_linker_tRNA and 5′scaff_NotI_3′tRNA, and NotI_5′gRNA scaff and 3′HDV_AvrII_5′ScCYCIt R. This modified TGR cassette was cloned into pDBtgr-Cas9 linearized with AvrII using NEB Hifi DNA Assembly, yielding pDBtdgr-Cas9. Insertion of the *HIS3* and *LEU2* target sites into pDBtdgr-Cas9 required PCR using the *HIS3* gRNA target insert F primer and the *LEU2* target insert R primer. This PCR product was then cloned into pDBtdgr-Cas9 digested with NheI and NotI, creating pDBtdgr-Cas9-HIS3-LEU2.

The RNAP III gRNA expression plasmids used to compare performance to our RNAP II TGR system were constructed through modification of pIW601. The $RPR1p_{Km}$-$tRNAgly_{Km}$-gRNA (RNAP III TG) cassette was produced by NEBuilder Hifi DNA Assembly of a double stranded oligo, generated by annealing HIS3 gRNA insert F and HIS3 gRNA insert R, into the PspXI site of pIW601; results in addition of a 'G' at the 5′ end of the scaffold tracrRNA as is present on pDBtgr-Cas9, and consistent with literature (DiCarlo et al., 2013; Juergens et al., 2018; Mali et al., 2013). The $RPR1p_{Km}$-$tRNAgly_{Km}$-gRNA-HDV ribozyme (RNAP III TGR) cassette was produced by PCR of the gRNA scaffold and HDV ribozyme from pDBtgr-Cas9, using primers 3′KmtRNAgly_NheI_5′scaff and pIW601_SUP4t_3′HDV, and then cloned into pIW601 (digested with PspXI and SacII) using NEBuilder Hifi DNA assembly. Insertion of the *HIS3* target sequence into the RNAP III TGR cassette was conducted using a double stranded oligo into the NheI site as above.

Donors used to splice out 241, 244, 207, and 236 base pairs of the *HIS3, LEU2*, *ZWF1*, and *GPD1* loci, respectively, (KO donors) were created by overlap extension of single stranded oligos (HIS3 KO F and HIS3 KO R; LEU2 KO F and LEU2 KO R; ZWF1 KO F and ZWF1 KO R; GPD1 KO F and GPD1 KO R) used at 2.5 μM each. The forward oligo of each pair is comprised of 40 base pairs homologous to a region upstream of the respective target site followed by up to 20 base pairs complementary to the 3' end of the reverse oligo. The reverse oligo is comprised only of 40 base pairs homologous to a region downstream of the respective target site. Donors used for integration of the $PGKIp_{Km}$-*2PS*-$CYCIt_{Sc}$ cassette at the *HIS3* and *LEU2* loci were amplified from pKD-P2PS (McTaggart et al., 2019) using primers 2PS int KmHIS3 F and 2PS int KmHIS3 R or KmPGKIp int LEU2 F and CYCIt int LEU2 R, respectively. To synthesize donor DNA comprised of the *K. marxianus ACC1* coding sequence under the control of a characterized promoter and terminator pair, the *ACC1* coding sequence was first amplified from CBS 712 genomic DNA using primers pCV842 ACC1 F and pCV842 ACC1 R. NEBuilder HiFi DNA Assembly was used to insert the amplified *ACC1* sequence into pCA-A (McTaggart et al., 2019) digested with SpeI and XhoI, yielding pCA-A-ACC1. The $ADH2p_{Sc}$-$ACC1_{Km}$-$CYCIt_{Sc}$ cassette was then amplified for integration into the *HIS3* and *LEU2* loci using primers ScADH2p int HIS3 F and 2PS int KmHIS3 R or ScADH2p int LEU2 F and CYCIt int LEU2 R, respectively. A small sample of each donor DNA PCR reaction was verified for synthesis of the correctly sized product by gel electrophoresis, after which the remaining volume of the PCR reaction was purified using the DNA Clean & Concentrator Kit (Zymo Research, Irvine, CA).

2.3. Transformation of K. marxianus for genomic modification

K. marxianus strains were streaked from frozen glycerol stocks onto YPD and incubated at 30 °C for 48–72 h. Single colonies were then inoculated into 3 mL YPD, grown overnight at 30 °C and 250 rpm in an air incubator shaker (New Brunswick Scientific Co. Excella E25, Edison, NJ), reinoculated to OD_{600} 0.5 (Shimadzu UV-2450 UV–Vis Spectrophotometer, Columbia, MD) in fresh 3 mL YPD media per transformation, and grown for approximately 4 h at 30 °C until OD_{600} 2.0 was reached. The Frozen-EZ Yeast Transformation II Kit (Zymo Research, Irvine, CA) was utilized for all plasmid transformations with the following minor modifications. The volumes of Frozen-EZ Solution I, II, and III used per transformation was 250, 50, and 250 μL, respectively. For transformations involving CRISPR-related plasmids, after addition of Frozen-EZ Solution II, 10 μL of 10 mg/mL sheared salmon sperm DNA (Invitrogen, Waltham, MA) – previously boiled at 95 °C for 5 min and

immediately cooled on ice – was added to each reaction. Where applicable, donor DNA was added prior to plasmid DNA to the amount of 650 ng for KO donors or 1 μg for all others. Plasmid DNA was always added to the amount of 500 ng. After addition of Frozen-EZ Solution III, transformation reactions were incubated at 30 °C for 2 h before plating onto SDCA medium. Transformations involving CRISPR-related plasmids required about 36 h before colonies were apparent on plates, about 12 h longer than other plasmid transformations. When an outgrowth was implemented after the 2-h incubation at 30 °C, the transformation reaction was transferred to a culture tube, spun at 500×*g* for 2 min in an Allegra X-22R centrifuge (Beckman Coulter, Brea, CA), and the supernatant was replaced with 3 mL SDCA. Cultures were then cultivated at 30 °C for 2 days before plating onto SDCA.

2.4. Genotype analysis of targeted loci

All targeted loci were evaluated for successful integration through colony PCR of transformants using OneTaq DNA Polymerase (New England BioLabs, Ipswich, MA). Analysis at each locus, regardless of type of donor transformed, involved two primers that bind externally to the donor homology sequences (*HIS3:* KmHIS3 upstream donor F and KmHIS3 downstream donor R; *LEU2*: KmLEU2 int check F and KmLEU2 int check R; *ZWF1:* ZWF1 check F and ZWF1 check R; *GPD1*: GPD1 check F and GPD1 check R). When analyzing colonies transformed with a 2PS or ACC1 donor, an additional primer binding internal to the donor sequence was also included (2PS 650up F or ACC1 int F2). In all cases, the selected set of primers enable simultaneous resolution of the wild-type and integrated genotypes for detection of heterogeneous transformants. Representative images of gel electrophoresis analysis for these PCRs are depicted in Fig. S1. Expected PCR product sizes at the *HIS3* and *LEU2* loci for each donor evaluated, and for all possible combinations of repair by homologous recombination and non-homologous end joining using a single donor fragment, are listed in Table S3. When determining percent integration, transformants revealed to be homogeneous for the desired integration as well as those detected to be heterogeneous were counted as successful integrations.

To check for gene KOs through the formation of indels by non-homologous end joining, transformants were first restreaked on SDCA and grown at 37 °C for 36 h to eliminate heterogeneous colonies. Three daughter colonies were chosen at random per original transformant and restreaked onto an SD-HIS or SD-LEU plate for colonies transformed with pDBtgr-Cas9-HIS3 or pDBtgr-Cas9-LEU2, respectively, and grown at 37 °C overnight. A lack of growth on SD-HIS or SD-LEU paired with lack of an integration-positive PCR result, where appropriate, was taken as sufficient evidence of a successful KO of *HIS3* or *LEU2* by NHEJ.

2.5. Knockout of KU70 Gene

To knockout the *KU70* gene in strain CBS 712Δ*U*, a *URA3* blaster (Alani et al., 1987) integrating vector was utilized (this effort occurred in parallel to construction of our CRISPR system). This KU70-URAblaster vector was built as described by Mctaggart (2020), except the homology sequences were extended to 777 and 763 base pairs, creating KU70-UBV2. KU70-UBV2 was digested with XhoI and XbaI to remove unnecessary sequences prior to transforming 800 ng of the isolated fragment using the Zymo Frozen-EZ Yeast Transformation II kit as above, except transformation reactions were incubated for three hours at 30 °C prior to plating. Integration of the KU70-UBV2 fragment was selected for on SDCA plates. Transformants were screened by colony PCR using three primers (KU70 External F, KU70 Plas REV, and URA seq Rev) to simultaneously check for target and off-target integration. Upon identification of a correctly targeted transformant, the *URA3* selection marker was excised by inoculating the transformant into 3 mL YPD for 24 h followed by two 24-h cultivations in 3 mL YPD supplemented with 1 g/L 5-FOA. Cultures were then plated on YPD for single colonies and evaluated by colony PCR for loss of *URA3* (Fig. S2).

2.6. TAL biosynthesis and quantification

Engineered strains were re-streaked onto SDCA after transformation to eliminate heterogenous colonies. Loss of the pDBtgr-Cas9 plasmid was achieved through 5-FOA treatment as above. Strains were then transformed with pKD-P2PS and stored as frozen glycerol stocks. In preparation for the TAL studies, strains were streaked onto SDCA plates and grown for 2.5 days at 37 °C. Individual colonies were then inoculated into 3 mL SXCA or SLCA media. After 2 days, each strain was reinoculated to OD_{600} 0.1 in 3 mL of the same medium and grown at 37 °C for 48 h in a Gyromax 929 Water Bath Shaker (Amerex Instruments, Inc., Concord, CA). OD_{600} was then measured, cultures were spun down at 2,600×*g* for 4 min (Allegra X-22R Centrifuge, Beckman Coulter, Brea, CA), and a sample of the supernatant was collected and stored at 4 °C until measurement. Samples were prepared and measured for TAL titer using a plate reader (SpectraMax M3, Molecular Devices) as previously described by Lang et al. (2020).

3. Results and discussion

3.1. Design of a high efficiency CRISPR system for K. marxianus

For metabolic engineering of *K. marxianus*, a high efficiency CRISPR system using donors with short (40 bp) homology arms and no selection marker, minimal DNA input, and no extended outgrowth period would be very advantageous. The flexibility to work in wild-type NHEJ-functional strains is also desirable. To enable this, we constructed plasmid pDBtgr-Cas9 by replacing the RNAP III-driven gRNA expression cassette of pIW601 (a CEN/ARS plasmid harboring a codon-optimized Cas9 gene (Löbs et al., 2017)) with a TGR cassette (Fig. 1) under the control of the strong and constitutive RNAP II promoter P_{TDH3} from *S. cerevisiae*. The promoter was followed by the *K. marxianus* glycine tRNA, an NheI restriction site for target site insertion, tracrRNA, HDV ribozyme, and *CYC1* terminator from *S. cerevisiae.* Upon the nucleolytic activity of RNase Z to remove the 5′ tRNA (Schiffer et al., 2002) and the self-cleaving activity of the 3′ HDV ribozyme (Ferré-D'Amaré and Scott, 2010), a mature gRNA transcript is produced. Design of the TGR cassette was inspired by work conducted by Ng and Dean (2017) who showed significantly better performance of a TGR cassette over a hammer head ribozyme-gRNA-HDV ribozyme (RGR) cassette in *Candida albicans*. Such an RGR cassette has previously been used in *K. marxianus* with success in creating gene KOs, demonstrating a 24% integration efficiency of a donor comprised solely of 959 bp homology to the *ADE2* locus in a NHEJ-functional strain (Juergens et al., 2018), or using a 160 bp KO donor for disruption of *ARO8* (Rajkumar and Morrissey, 2022).

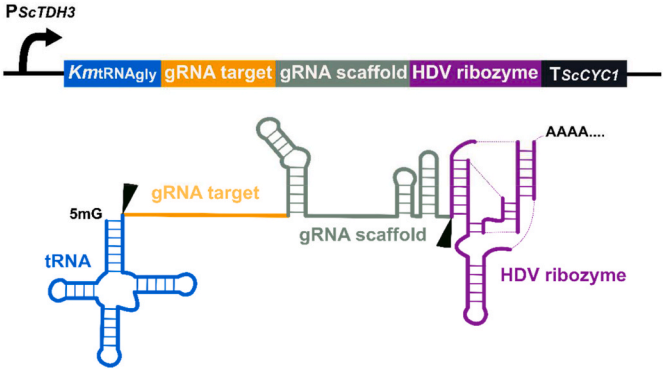

Fig. 1. TGR gene cassette and approximate premature transcript secondary structure. Black triangles indicate sites of tRNA and HDV ribozyme cleavage.

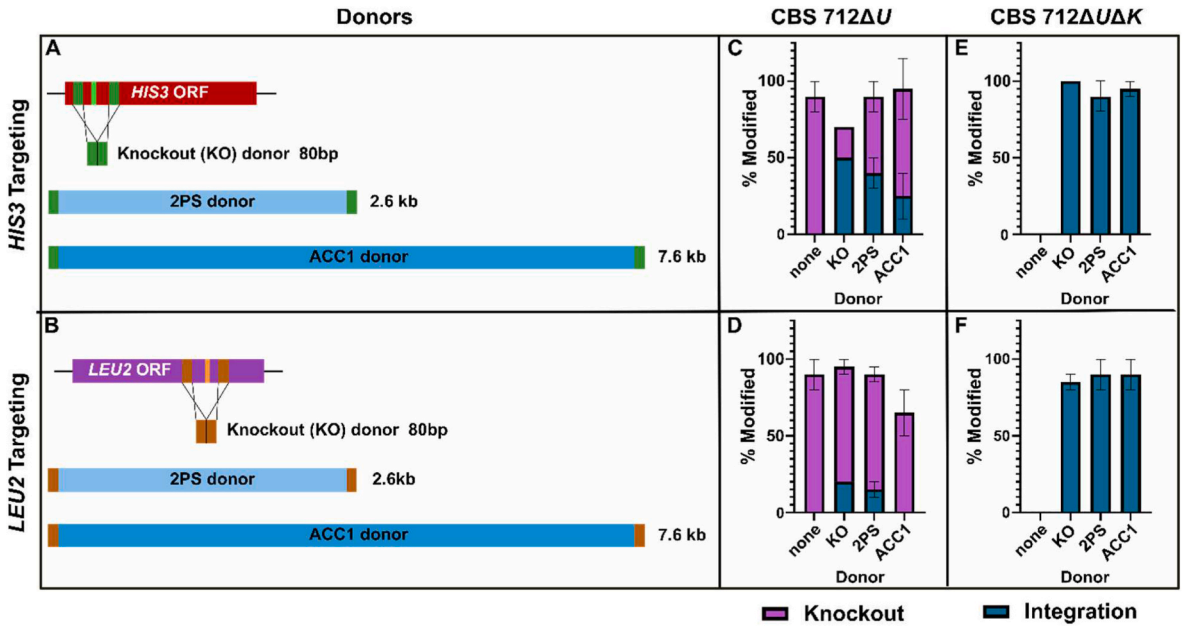

Fig. 2. CRISPR-mediated genome modification in *K. marxianus*. **A, B** The *HIS3* and *LEU2* loci were targeted using pDBtgr-Cas9 plasmids containing 20 bp targeting sequences matching locations within each ORF (*HIS3*: bright green band; *LEU2*: bright orange band). Integration of three different donors were evaluated, an 80 bp KO donor, a *g2ps1* expression cassette, and an *ACC1* expression cassette, each containing 40 bp homology sequences matching regions of the targeted ORF just upstream and downstream of the targeting sequence (*HIS3*: dark green; *LEU2*: dark orange). **C, D** Percentage of transformants with a gene knockout or donor integration in a NHEJ-functional strain, CBS 712Δ*U* and **E,F** in a NHEJ-deficient strain, CBS 712Δ*U*Δ*K*. The total height of the bars represents average total gene knockout frequency ± standard deviation and the height of the blue bars represents the proportion of KOs that were created through integration of a donor ± standard deviation. Ten transformants were analyzed for each of two transformations per condition. Unpaired t-tests showed there is no significant difference in the percent integration efficiency for the CBS 712Δ*U* strain when *HIS3* is targeted and co-transformed with the KO, 2PS, or ACC1 donor (panel C, three blue bars), nor when *LEU2* is targeted and co-transformed with the KO or 2PS donor (panel D, two blue bars). (For interpretation of the references to colour in this figure legend, the reader is referred to the Web version of this article.)

3.2. Gene disruption and integration in wild-type and NHEJ-deficient strains

The function of our new RNAP II gRNA expression system was evaluated through targeting of the *HIS3* and *LEU2* open reading frames (ORF) for gene knockout (KO) and various gene integrations. Twenty base pair targeting sequences matching regions for each of these ORFs were cloned into pDBtgr-Cas9, creating pDBtgr-Cas9-HIS3 and pDBtgr-Cas9-LEU2. We chose a range of repair fragment sizes to determine the effect of insert size on efficiency and restricted the homology sequences to 40 bp per arm. Each plasmid was transformed into CBS 712Δ*U* alone or with one of three different linear DNA repair fragments (Fig. 2A and B) and transformants were selected on uracil-deficient plates. The first was an 80 bp fragment (KO donor) comprised of the fusion of two 40 base pair homology sequences matching regions just upstream and just downstream of the respective target site; this results in removal of approximately 240 base pairs from the ORF when integrated by homologous recombination. The second and third fragments contain the same 40 bp homology sequences flanking either a 2.6 kb expression cassette ($PGKIp_{Km}$-*g2ps1*-$CYCIt_{Sc}$) or a 7.6 kb cassette ($ADH2p_{Sc}$-$ACC1_{Km}$-$CYCIt_{Sc}$). The *g2ps1* gene is from *Gerbera hybrida* and codes for 2-pyrone synthase (2-PS) for the synthesis of the polyketide triacetic acid lactone (Eckermann et al., 1998). The *K. marxianus ACC1* gene codes for acetyl-CoA carboxylase, the enzyme responsible for conversion of acetyl-CoA to malonyl-CoA, a reaction important for fatty acid biosynthesis as well as polyketide bioproduction (Choi and Da Silva, 2014).

We first evaluated editing efficiency in a *K. marxianus* strain with native NHEJ activity. Transformants were re-streaked onto SDCA to obtain homogeneous colonies. When these daughter colonies were streaked onto histidine- or leucine-deficient plates, 65–95% failed to grow indicating successful gene knockout through creation of an indel by NHEJ or integration of the repair fragment (Fig. 2C and D; purple bars). Colony PCR of these transformants revealed substantial levels of repair fragment integration at the *HIS3* site (Fig. 2C; blue bars). For transformations targeting the *LEU2* locus, integration efficiencies were less than those for the *HIS3* locus despite similar levels of gene knockout. This indicates high activity of the gRNAs in producing double stranded DNA cuts but differential rates of homology-directed repair (HDR) that may be improved through optimization of homology sequence design.

To improve the frequency of donor integration, we knocked out the native *KU70* gene, encoding a member of the KU70/KU80 heterodimer responsible for the first step of the NHEJ pathway (Chang et al., 2017), creating strain CBS 712Δ*U*Δ*K*. We first evaluated the effect of *KU70* KO on NHEJ activity by transforming pDBtgr-Cas9-HIS3 and pDBtgr-Cas9-LEU2 in the absence of donor. For such transformations conducted in a NHEJ-deficient strain, it is expected that minimal transformants will develop since successful double-stranded DNA breaks will result in cell death. Indeed, less than five colonies appeared on a plate for each transformation, a >1000-fold drop in the number of transformants compared to transformation of the non-targeting plasmid, and each of these few transformants were all shown to maintain *HIS3* or *LEU2* activity. This result indicates KO of *KU70* sufficiently inactivated the NHEJ pathway in CBS 712. To evaluate the effect of NHEJ inactivation on integration, the same set of transformations performed on CBS 712Δ*U* above were performed in this NHEJ-deficient strain. For all conditions in which a donor was co-transformed, exceptionally high rates of integration were achieved, approaching 100% for all donors evaluated regardless of donor size or locus targeted (Fig. 2E and F). Furthermore, KO of *KU70* offered significantly enhanced selection of transformants engineered through HDR with particularly improved performance for the large *ACC1* donor over the NHEJ-functional strain.

It has been reported that knockout of *KU70* or other genes involved in the NHEJ pathway can hinder the fitness of a strain due to their shared role in telomere maintenance (Liti and Louis, 2003; Polotnianka et al.,

1998). The deleterious effects of NHEJ gene knockouts on strain fitness has been demonstrated in some yeasts including *S. cerevisiae* (Palmbos et al., 2005) and *S. stipitis* (Ploessl et al., 2021). However, comparison of the growth rate of CBS 712Δ*U* and CBS 712Δ*U*Δ*K* grown in YPD at 37 °C revealed no significant differences between the two strains (Fig. S3). This is consistent with work completed by Choo et al. (2014) which demonstrated that knockout of *KU80* in *K. marxianus* KCTC 17555 did not decrease cell fitness under normal and several environmentally stressful conditions. Knockout of *KU70* has the additional benefit of limiting the propensity for random integration events compared to when NHEJ is functional (Abdel-Banat et al., 2009; Rajkumar et al., 2019), facilitating more predictable engineering outcomes.

For a direct comparison with RNAP III-driven systems, we performed the same experiments (using the *HIS3* locus) with two RNAP III-driven systems: *RPR1p*$_{Km}$-*tRNAgly*$_{Km}$-gRNA (RNAP III TG) and *RPR1p*$_{Km}$-*tRNAgly*$_{Km}$-gRNA-HDV ribozyme (RNAP III TGR). The RNAP II TGR system outperformed both RNAP III systems, particularly for gene integrations (Fig. S4). This data agrees with work conducted in *Candida albicans* comparing the efficiency of various RNAP II and RNAP III gRNA expression systems (Ng and Dean, 2017). Overall, the high efficiency of our RNAP II-driven TGR expression cassette provides a significant improvement over the existing *K. marxianus* tools summarized in Table S1. The ability to successfully use donors with only 40 bp homology sequences greatly simplifies donor synthesis since such overhangs can be added through a straight-forward, single-step PCR process. Many other demonstrations of CRISPR-Cas9-mediated gene integrations in *K. marxianus* have used donors with large homology sequences 0.7–0.9 kb in length which requires multi-step PCR processes and are sometimes cloned into vectors (Cernak et al., 2018; Li et al., 2021). Our system was also able to achieve high genomic modification efficiencies with minimal DNA input, only requiring 500 ng of plasmid and up to 1 μg of linear donor; other studies used several micrograms of each, up to 10 μg plasmid and 5 μg donor (Cernak et al., 2018; Nambu-Nishida et al., 2017, 2018). Our work also demonstrates the largest, single genomic integration (7.6 kb for *ACC1*) achieved through CRISPR-Cas9 without selection in *K. marxianus*, and with near 100% integration efficiency in the *KU70* KO strain. Prior studies achieved integrations of 3.5 kb or less, not including the often lengthy homology sequences (Cernak et al., 2018; Juergens et al., 2018; Li et al., 2021; Nambu-Nishida et al., 2017, 2018; Rajkumar and Morrissey, 2020). The factors above make our system significantly easier to use, while also offering greater efficiency, the flexibility to use NHEJ-functional and NHEJ-deficient *K. marxianus* strains, and the ability to integrate genes of varying lengths.

3.3. Selection of growth-biased metabolic engineering modifications for enhanced polyketide biosynthesis

Previously characterized CRSIPR-Cas9 systems for *K. marxianus* (Cernak et al., 2018; Li et al., 2021) as well as other yeasts (Bao et al., 2015; Horwitz et al., 2015; Schwartz et al., 2017) often compensate for lower gRNA-targeting efficiency and low HDR rates by incorporating liquid outgrowth periods in selective media before plating and assaying for the engineered strains. While proven to increase the efficiency of integration in these studies, this method can fail to yield the desired strains if the modification significantly reduces cell growth rate. As previously demonstrated by Schwartz et al. (2017), such mutants are unlikely to be recovered after an outgrowth where the unedited, faster growing cells can vastly outnumber the slower growing mutants in just a few generations. A CRISPR-Cas9 system with universal metabolic engineering utility should allow for selection of gene modifications that potentially reduce cell fitness.

To demonstrate the ability of our new RNAP II system to select strains with reduced cell fitness without use of a liquid outgrowth period, we disrupted the genes for glucose-6-phosphate 1-dehydrogenase (*ZWF1*), the enzyme catalyzing the first step of the pentose phosphate pathway, and glycerol-3-phosphate dehydrogenase (*GPD1*), the enzyme that sequesters carbon away from glycolysis toward the biosynthesis of glycerol. Knockout of *ZWF1* is known to cause growth defects in *K. marxianus* due to impaired regeneration of NADPH (Zhang et al., 2020b); however, loss of carbon in the oxidative phase of the pentose phosphate pathway has been shown to make this gene knockout advantageous for improving the titer of triacetic acid lactone (Cardenas and Da Silva, 2014) and ethanol (Verho et al., 2003) in *S. cerevisiae*. Knockout of *GPD1* has similarly been shown to cause growth defects in *K. marxianus* (Zhang et al., 2020a), but has also assisted in elevated ethanol accumulation in an engineered *K. marxianus* strain (Zhang et al., 2015).

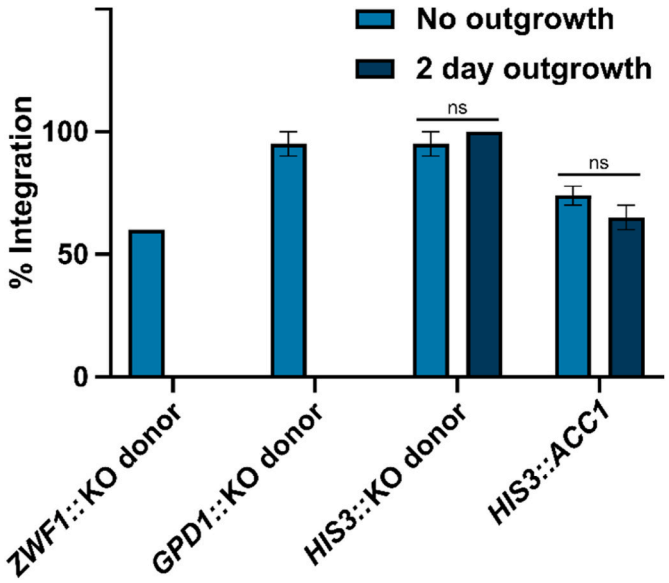

Fig. 3. Comparison of gene integration frequency in CBS 712Δ*U*Δ*K* with and without use of a two-day outgrowth prior to plating. Acquisition of four different modifications were evaluated using each post-transformation method. The missing bar for the *ZWF1*::KO donor and *GPD1*::KO donor conditions is indicative of the lack of recovery of any *ZWF1* KO and *GPD1* KO mutants, respectively, after use of a two-day outgrowth prior to plating. Bars represent the average frequency of integration for the respective donor ± standard deviation. Ten transformants were analyzed for each of two transformations per condition.

Strain CBS 712Δ*U*Δ*K* was transformed with pDBtgr-Cas9-ZWF1 or pDBtgr-Cas9-GPD1 along with a corresponding 80 bp KO donor and plated immediately after transformation. Screening via colony PCR showed that an average of 60% or 95% of colonies exhibited the desired *ZWF1* or *GPD1* KO, respectively (Fig. 3). However, when the cells were instead inoculated into selective SDCA media and cultured for two days before plating, all ten colonies from each of two biological replicates had the native *ZWF1* or *GPD1* genotype. The cells with targeted gene disruptions were lost during the multi-day outgrowth period due to their significantly slower growth rates relative to the cells that evaded editing (Fig. S5). For comparison, in similar transformations targeting the *HIS3* locus with either the 80 bp KO donor or the *ACC1* donor (modifications that do not result in a substantial change in growth rate (Fig. S5)), plating immediately after transformation or after a two-day outgrowth resulted in no significant change in integration efficiency (Fig. 3). This study demonstrates that the use of a higher efficiency CRISPR-Cas9 system such as pDBtgr-Cas9 makes outgrowth unnecessary. This is vital for recovery of engineered strains with even marginal growth defects that can be lost due to growth-bias during a liquid outgrowth period. Even though outgrowth was found to be unnecessary using pDBtgr-Cas9 plasmids, it is noted that re-streaking of transformants is often necessary to isolate homogenous colonies before moving forward with plasmid curing and any subsequent transformations. As described previously by Ng and Dean (2017) and Schwartz et al. (2017),

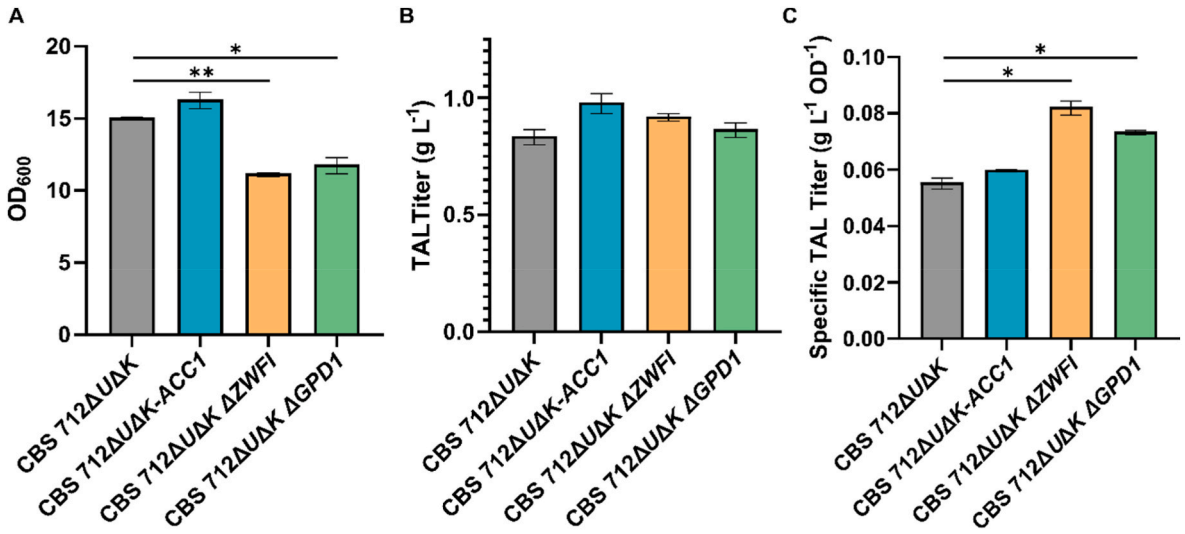

Fig. 4. Growth and TAL production from unengineered and engineered *K. marxianus* strains grown for 48 h in 3 mL SLC media at 37 °C. All strains harbor the higher-copy pKD-P2PS plasmid. **A** Growth (optical density at 600 nm). **B** TAL titer. **C** Specific TAL Titer. Bars represent average ± standard deviation for 2 biological replicates, *p < 0.05, **p < 0.01. TAL: triacetic acid lactone.

heterogeneous colonies are common if plating immediately after transformation since editing may not occur until after a number of cell divisions.

To demonstrate the importance of eliminating this growth bias for metabolic engineering, we evaluated the resulting strains for improved carbon flux to a desired product in *K. marxianus*. CBS 712Δ*UΔK ΔZWF1*, CBS 712Δ*GPD1*, and CBS *712ΔUΔK-ACC1* were transformed with pKD-P2PS (McTaggart et al., 2019) to enable production of triacetic acid lactone, a simple polyketide with promising utility as a precursor to several commodity and higher-value products (Chia et al., 2012; Shanks and Keeling, 2017). The three strains were cultured in synthetic defined media supplemented with 9.5 g/L lactose (SLCA) for 48 h at 37 °C. Despite the growth impact, the *ZWF1* KO strain had a significant increase in average specific TAL titer (0.92 g/L, 0.082 g/L/OD), 48% higher than the wild-type strain (0.84 g/L, 0.056 g/L/OD) (Fig. 4). The *GPD1* KO strain exhibited similar behavior as the *ZWF1 KO*, producing an increase in average specific TAL titer (0.87 g/L, 0.074 g/L/OD) over the unmodified strain. The ability of our pDBtgr-Cas9 system to facilitate selection of genome modifications, including those resulting in reduced *K. marxainus* growth rate, provides opportunities to test a broader range of metabolic engineering interventions that may result in beneficial phenotypes.

3.4. Expanding the TGR cassette for simultaneous integrations at multiple loci

Due to the exceptionally high efficiency of our RNAP II-driven TGR cassette for integrating one construct of varying size at a single genomic

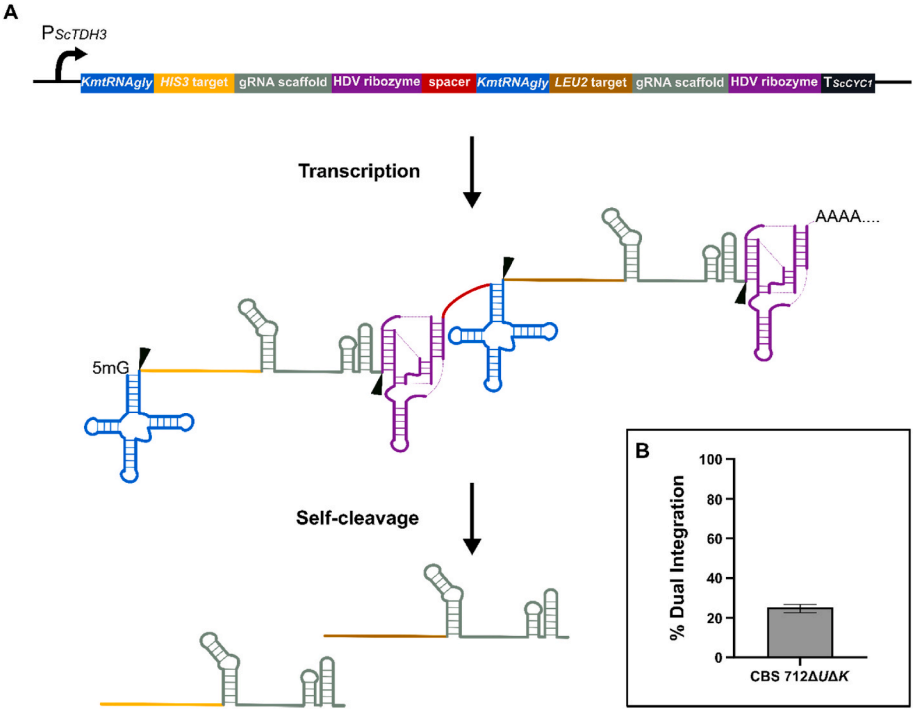

Fig. 5. Expansion of TGR cassette for simultaneous targeting of two loci in *K. marxianus*. **A** Double gRNA cassette structure, approximate pre-mature transcript secondary structure, and final gRNAs after self-cleavage at the black triangles. **B** Percentage of transformations with simultaneous, dual integrations at the *HIS3* and *LEU2* loci in *K. marxianus* using *ACC1* and *g2ps1* gene donors, respectively. Bar represents average ± standard deviation of two experiments comprised of two and four transformations, with up to ten transformants analyzed per transformation.

site, we adapted our system for simultaneous modification of two (and potentially more) sites in the genome. pDBtgr-Cas9 was modified to express more than one gRNA through insertion of an additional tRNA-gRNA-HDV ribozyme cassette immediately downstream of the original TGR sequence, separated by a short spacer sequence (Fig. 5A), yielding plasmid pDBtDgr-Cas9. Expression of this cassette will result in one long transcript containing two gRNAs; however, self-cleaving activity of the tRNAs and HDV ribozymes will ultimately result in two mature and independent gRNAs.

To evaluate the efficiency of this dgRNA cassette, targeting sequences for *HIS3* and *LEU2* were inserted into the pDBtDgr-Cas9 backbone using a single-step Gibson assembly process, forming plasmid pDBtDgr-Cas9-HIS3-LEU2. This plasmid was transformed as before into the NHEJ-deficient strain CBS 712Δ*U*Δ*K* with the *ACC1* donor containing 40 bp homologies to the *HIS3* locus as well as the *2PS* donor containing 40 bp homologies to the *LEU2* locus. Across two independent experiments, the average percent of transformants with the desired dual integrations was 25.5% (Fig. 5B).

Others have been successful at integrating more than one gene into a single site in *K. marxianus*, but the strategies required use of either complex PCR schemes to assemble multiple genes into a single donor fragment with very large homology sequences (Li et al., 2021), or required simultaneous integration of a selection marker (Chang et al., 2012; Ha-Tran et al., 2021; Lee et al., 2020; Lin et al., 2017). This study marks the first demonstration of dual markerless integrations at multiple sites in *K. marxianus*. Furthermore, only 40 bp homology regions were used and no selection marker was required. By enabling simultaneous editing at two sites in the genome, the double gRNA system described here can expedite *K. marxianus* strain engineering by consolidating rounds of the time-consuming transformation, mutation verification, and plasmid curing processes by one half. The system also has the potential for expansion to more than two simultaneous integrations by concatenating additional tRNA-gRNA-HDV cassettes. This is an important contribution to the set of genetic tools available for efficient metabolic engineering of *K. marxianus*, potentially opening the door to the study of a broader set of pathways and biorenewable products in this industrially advantageous host.

4. Conclusions

The development of this highly efficient CRISPR-Cas9 system offers a streamlined platform for expedited strain engineering in *K. marxianus* by eliminating the need for complex donor assemblies, eliminating extended outgrowth periods, and allowing multiplexed gene editing with the flexibility for use in both NHEJ-functional and -deficient strains. This system provides a powerful addition to the synthetic biology toolbox for metabolic engineering of *K. marxianus*, further advancing this yeast as a promising candidate for extensive industrial biomanufacturing.

CRediT authorship contribution statement

Danielle Bever: Conceptualization, Methodology, Investigation, Writing – original draft. **Ian Wheeldon:** Writing – review & editing, Funding acquisition, Project administration. **Nancy Da Silva:** Conceptualization, Methodology, Writing – review & editing, Supervision, Project administration, Funding acquisition.

Declaration of competing interest

The authors declare that they have no known competing financial interests or personal relationships that could have appeared to influence the work reported in this paper.

Data availability

Data will be made available on request.

Acknowledgements

This research was supported by the National Science Foundation [grant numbers CBET-1803677 (NDS) and CBET-1803630 (IW)] and the U.S. Department of Energy, Office of Science, Office of Biological and Environmental Research, Genomic Science Program [grant number SC0019093 (IW and NDS)]. The authors would like to thank Tami McTaggart for her helpful advice and Shane Bassett for his general experimental support and writing assistance.

Appendix A. Supplementary data

Supplementary data to this article can be found online at https://doi.org/10.1016/j.mec.2022.e00208.

References

Abdel-Banat, B.M.A.A., Nonklang, S., Hoshida, H., Akada, R., 2009. Random and targeted gene integrations through the control of non-homologous end joining in the yeast *Kluyveromyces marxianus*. Yeast 27. https://doi.org/10.1002/yea.1729 n/a-n/a.

Alani, E., Cao, L., Kleckner, N., 1987. A method for gene disruption that allows repeated use of URA3 selection in the construction of multiply disrupted yeast strains. Genetics 116, 541–545. https://doi.org/10.1534/genetics.112.541.test.

Altschul, S.F., Gish, W., Miller, W., Myers, E.W., Lipman, D.J., 1990. Basic local alignment search tool. J. Mol. Biol. 215, 403–410. https://doi.org/10.1016/S0022-2836(05)80360-2.

Amrane, A., Prigent, Y., 1998. Effect of culture conditions of Kluyveromyces marxianus on its autolysis, and process optimization. Bioprocess Eng. 18, 383–388. https://doi.org/10.1007/pl00008998.

Banat, I.M., Nigam, P., Marchant, R., 1992. Isolation of thermotolerant, fermentative yeasts growing at 52°C and producing ethanol at 45°C and 50°C. World J. Microbiol. Biotechnol. 8, 259–263. https://doi.org/10.1007/BF01201874.

Bao, Z., Xiao, H., Liang, J., Zhang, L., Xiong, X., Sun, N., Si, T., Zhao, H., 2015. Homology-integrated CRISPR–cas (HI-CRISPR) system for one-step multigene disruption in *Saccharomyces cerevisiae*. ACS Synth. Biol. 4, 585–594. https://doi.org/10.1021/sb500255k.

Benchling, 2021. Benchling [Biology Software].

Cardenas, J., Da Silva, N.A., 2014. Metabolic engineering of Saccharomyces cerevisiae for the production of triacetic acid lactone. Metab. Eng. 25, 194–203.

Cernak, P., Estrela, R., Poddar, S., Skerker, J.M., Cheng, Y.-F., Carlson, A.K., Chen, B., Glynn, V.M., Furlan, M., Ryan, O.W., Donnelly, M.K., Arkin, A.P., Taylor, J.W., Cate, J.H.D., 2018. Engineering *Kluyveromyces marxianus* as a robust synthetic biology platform host. mBio 9. https://doi.org/10.1128/mBio.01410-18.

Chang, H.H.Y., Pannunzio, N.R., Adachi, N., Lieber, M.R., 2017. Non-homologous DNA end joining and alternative pathways to double-strand break repair. Nat. Rev. Mol. Cell Biol. https://doi.org/10.1038/nrm.2017.48.

Chang, J.J., Ho, C.Y., Ho, F.J., Tsai, T.Y., Ke, H.M., Wang, C.H.T., Chen, H.L., Shih, M.C., Huang, C.C., Li, W.H., 2012. PGASO: a synthetic biology tool for engineering a cellulolytic yeast. Biotechnol. Biofuels 5, 1–12. https://doi.org/10.1186/1754-6834-5-53/FIGURES/5.

Charoensopharat, K., Thanonkeo, P., Thanonkeo, S., Yamada, M., 2015. Ethanol production from Jerusalem artichoke tubers at high temperature by newly isolated thermotolerant inulin-utilizing yeast Kluyveromyces marxianus using consolidated bioprocessing. Antonie van Leeuwenhoek, Int. J. Gen. Mol. Microbiol. 108, 173–190. https://doi.org/10.1007/S10482-015-0476-5/TABLES/10.

Chia, M., Schwartz, T.J., Shanks, B.H., Dumesic, J.A., 2012. Triacetic acid lactone as a potential biorenewable platform chemical. Green Chem. 14, 1850–1853. https://doi.org/10.1039/c2gc35343a.

Choi, J.W., Da Silva, N.A., 2014. Improving polyketide and fatty acid synthesis by engineering of the yeast acetyl-CoA carboxylase. J. Biotechnol. 187, 56–59. https://doi.org/10.1016/J.JBIOTEC.2014.07.430.

Choo, J.H., Han, C., Kim, J.Y., Kang, H.A., 2014. Deletion of a KU80 homolog enhances homologous recombination in the thermotolerant yeast Kluyveromyces marxianus. Biotechnol. Lett. 36, 2059–2067. https://doi.org/10.1007/S10529-014-1576-4/TABLES/2.

DiCarlo, J.E., Norville, J.E., Mali, P., Rios, X., Aach, J., Church, G.M., 2013. Genome engineering in Saccharomyces cerevisiae using CRISPR-Cas systems. Nucleic Acids Res. 41, 4336–4343. https://doi.org/10.1093/nar/gkt135.

Doench, J.G., Fusi, N., Sullender, M., Hegde, M., Vaimberg, E.W., Donovan, K.F., Smith, I., Tothova, Z., Wilen, C., Orchard, R., Virgin, H.W., Listgarten, J., Root, D.E., 2016. Optimized sgRNA design to maximize activity and minimize off-target effects of CRISPR-Cas9. Nat. Biotechnol. 342 34, 184–191. https://doi.org/10.1038/nbt.3437, 2015.

Eckermann, S., Schröder, G., Schmidt, J., Streck, D., Edrada, R.A., Helariutta, Y., Elomaa, P., Kotilainen, M., Kilpeläinen, I., Proksch, P., Teeri, T.H., Schröder, J.,

1998. New pathway to polyketides in plants. Nature 396, 387–390. https://doi.org/10.1038/24652.
Ferré-D'Amaré, A.R., Scott, W.G., 2010. Small self-cleaving ribozymes. Cold Spring Harbor Perspect. Biol. 2, a003574. https://doi.org/10.1101/cshperspect.a003574.
Fonseca, G.G., De Carvalho, N.M.B., Gombert, A.K., 2013. Growth of the yeast Kluyveromyces marxianus CBS 6556 on different sugar combinations as sole carbon and energy source. Appl. Microbiol. Biotechnol. 97, 5055–5067. https://doi.org/10.1007/s00253-013-4748-6.
Fonseca, G.G., Gombert, A.K., Heinzle, E., Wittmann, C., 2007. Physiology of the yeast Kluyveromyces marxianus during batch and chemostat cultures with glucose as the sole carbon source. FEMS Yeast Res. 7, 422–435. https://doi.org/10.1111/j.1567-1364.2006.00192.x.
Gao, Y., Zhao, Y., 2014. Self-processing of ribozyme-flanked RNAs into guide RNAs *in vitro* and *in vivo* for CRISPR-mediated genome editing. J. Integr. Plant Biol. 56, 343–349. https://doi.org/10.1111/jipb.12152.
Gorter de Vries, A.R., de Groot, P.A., van den Broek, M., Daran, J.-M.G., 2017. CRISPR-Cas9 mediated gene deletions in lager yeast Saccharomyces pastorianus. Microb. Cell Factories 16, 222. https://doi.org/10.1186/s12934-017-0835-1.
Groeneveld, P., Stouthamer, A.H., Westerhoff, H.V., 2009. Super life - how and why 'cell selection' leads to the fastest-growing eukaryote. FEBS J. 276, 254–270. https://doi.org/10.1111/j.1742-4658.2008.06778.x.
Ha-Tran, D.M., Lai, R.Y., Nguyen, T.T.M., Huang, E., Lo, S.C., Huang, C.C., 2021. Construction of engineered RuBisCO Kluyveromyces marxianus for a dual microbial bioethanol production system. PLoS One 16, e0247135. https://doi.org/10.1371/JOURNAL.PONE.0247135.
Hillman, E.T., Li, M., Hooker, C.A., Englaender, J.A., Wheeldon, I., Solomon, K.V., 2021. Hydrolysis of lignocellulose by anaerobic fungi produces free sugars and organic acids for two-stage fine chemical production with Kluyveromyces marxianus. Biotechnol. Prog. 37, e3172 https://doi.org/10.1002/BTPR.3172.
Horwitz, A.A., Walter, J.M., Schubert, M.G., Kung, S.H., Hawkins, K., Platt, D.M., Hernday, A.D., Mahatdejkul-Meadows, T., Szeto, W., Chandran, S.S., Newman, J.D., 2015. Efficient multiplexed integration of synergistic alleles and metabolic pathways in yeasts via CRISPR-cas. Cell Syst 1, 88–96. https://doi.org/10.1016/j.cels.2015.02.001.
Juergens, H., Varela, J.A., Gorter de Vries, A.R., Perli, T., Gast, V.J.M., Gyurchev, N.Y., Rajkumar, A.S., Mans, R., Pronk, J.T., Morrissey, J.P., Daran, J.-M.G., 2018. Genome editing in Kluyveromyces and Ogataea yeasts using a broad-host-range Cas9/gRNA co-expression plasmid. FEMS Yeast Res. 18 https://doi.org/10.1093/femsyr/foy012.
Ke, A., Ding, F., Batchelor, J.D., Doudna, J.A., 2007. Structural roles of monovalent cations in the HDV ribozyme. Structure 15, 281–287. https://doi.org/10.1016/J.STR.2007.01.017.
Kumar, P., Sahoo, D.K., Sharma, D., 2021. The identification of novel promoters and terminators for protein expression and metabolic engineering applications in Kluyveromyces marxianus. Metab. Eng. Commun. 12, e00160. https://doi.org/10.1016/j.mec.2020.e00160.
Lane, M.M., Morrissey, J.P., 2010. Kluyveromyces marxianus: a yeast emerging from its sister's shadow. Fungal Biol. Rev. 24, 17–26. https://doi.org/10.1016/j.fbr.2010.01.001.
Lang, X., Besada-Lombana, P.B., Li, M., Da Silva, N.A., Wheeldon, I., 2020. Developing a broad-range promoter set for metabolic engineering in the thermotolerant yeast Kluyveromyces marxianus. Metab. Eng. Commun., e00145 https://doi.org/10.1016/j.mec.2020.e00145.
Lee, M.E., DeLoache, W.C., Cervantes, B., Dueber, J.E., 2015. A highly characterized yeast toolkit for modular, multipart assembly. ACS Synth. Biol. 4, 975–986. https://doi.org/10.1021/sb500366v.
Lee, M.H., Lin, J.J., Lin, Y.J., Chang, J.J., Ke, H.M., Fan, W.L., Wang, T.Y., Li, W.H., 2018. Genome-wide prediction of CRISPR/Cas9 targets in Kluyveromyces marxianus and its application to obtain a stable haploid strain. Sci. Reports 8, 1–10, 2018 81. https://doi.org/10.1038/s41598-018-25366-z.
Lee, M.H., Hsu, T.L., Lin, J.J., Lin, Y.J., Kao, Y.Y., Chang, J.J., Li, W.H., 2020. Constructing a human complex type N-linked glycosylation pathway in Kluyveromyces marxianus. PLoS One 15, e0233492. https://doi.org/10.1371/JOURNAL.PONE.0233492.
Leonel, L.V., Arruda, P.V., Chandel, A.K., Felipe, M.G.A., Sene, L., 2021. Kluyveromyces Marxianus: a Potential Biocatalyst of Renewable Chemicals and Lignocellulosic Ethanol Production. https://doi.org/10.1080/07388551.2021.1917505 41, pp. 1131–1152. https://doi.org/10.1080/07388551.2021.1917505.
Li, M., Lang, X., Moran Cabrera, M., De Keyser, S., Sun, X., Da Silva, N., Wheeldon, I., 2021. CRISPR-mediated multigene integration enables Shikimate pathway refactoring for enhanced 2-phenylethanol biosynthesis in Kluyveromyces marxianus. Biotechnol. Biofuels 14, 1–15. https://doi.org/10.1186/S13068-020-01852-3/FIGURES/6.
Lin, Y.J., Chang, J.J., Lin, H.Y., Thia, C., Kao, Y.Y., Huang, C.C., Li, W.H., 2017. Metabolic engineering a yeast to produce astaxanthin. Bioresour. Technol. 245, 899–905. https://doi.org/10.1016/j.biortech.2017.07.116.
Liti, G., Louis, E.J., 2003. NEJ1 prevents NHEJ-dependent telomere fusions in yeast without telomerase. Mol. Cell. 11, 1373–1378. https://doi.org/10.1016/S1097-2765(03)00177-1.
Löbs, A.-K., Engel, R., Schwartz, C., Flores, A., Wheeldon, I., 2017. CRISPR–Cas9-enabled genetic disruptions for understanding ethanol and ethyl acetate biosynthesis in Kluyveromyces marxianus. Biotechnol. Biofuels 10, 164. https://doi.org/10.1186/s13068-017-0854-5.
Löbs, A.K., Schwartz, C., Thorwall, S., Wheeldon, I., 2018. Highly multiplexed CRISPRi repression of respiratory functions enhances mitochondrial localized ethyl acetate biosynthesis in Kluyveromyces marxianus. ACS Synth. Biol. 7, 2647–2655. https://doi.org/10.1021/acssynbio.8b00331.
Ma, H., Wu, Y., Dang, Y., Choi, J.-G., Zhang, J., Wu, H., 2014. Pol III promoters to express small RNAs: delineation of transcription initiation. Mol. Ther. Nucleic Acids 3, e161. https://doi.org/10.1038/mtna.2014.12.
Mali, P., Yang, L., Esvelt, K.M., Aach, J., Guell, M., DiCarlo, J.E., Norville, J.E., Church, G.M., 2013. RNA-guided human genome engineering via Cas9. Science 339, 823–826. https://doi.org/10.1126/SCIENCE.1232033/SUPPL_FILE/MALI.SM.PDF.
Marck, C., Kachouri-Lafond, R., Lafontaine, I., Westhof, E., Dujon, B., Grosjean, H., 2006. The RNA polymerase III-dependent family of genes in hemiascomycetes: comparative RNomics, decoding strategies, transcription and evolutionary implications. Nucleic Acids Res. 34, 1816. https://doi.org/10.1093/NAR/GKL085.
Martínez, O., Sánchez, A., Font, X., Barrena, R., 2018. Bioproduction of 2-phenylethanol and 2-phenethyl acetate by Kluyveromyces marxianus through the solid-state fermentation of sugarcane bagasse. Appl. Microbiol. Biotechnol. 102, 4703–4716. https://doi.org/10.1007/S00253-018-8964-Y/TABLES/3.
Mctaggart, T.L., 2020. Metabolic Engineering of Yeast to Maximize Precursor Formation and Polyketide Production by. UC Irvine.
McTaggart, T.L., Bever, D., Bassett, S., Da Silva, N.A., 2019. Synthesis of polyketides from low cost substrates by the thermotolerant yeast *Kluyveromyces marxianus*. Biotechnol. Bioeng. 116, 1721–1730. https://doi.org/10.1002/bit.26976.
Nambu-Nishida, Y., Nishida, K., Hasunuma, T., Kondo, A., 2018. Genetic and physiological basis for antibody production by Kluyveromyces marxianus. Amb. Express 8, 1–9. https://doi.org/10.1186/S13568-018-0588-1/FIGURES/4.
Nambu-Nishida, Y., Nishida, K., Hasunuma, T., Kondo, A., 2017. Development of a comprehensive set of tools for genome engineering in a cold- and thermo-tolerant Kluyveromyces marxianus yeast strain. Sci. Rep. 7, 8993. https://doi.org/10.1038/s41598-017-08356-5.
Ng, H., Dean, N., 2017. Dramatic improvement of CRISPR/Cas9 editing in Candida albicans by increased single guide RNA expression. mSphere 2, e00385. https://doi.org/10.1128/mSphere.00385-16, 16.
Nonklang, S., Abdel-Banat, B.M.A., Cha-aim, K., Moonjai, N., Hoshida, H., Limtong, S., Yamada, M., Akada, R., 2008. High-temperature ethanol fermentation and transformation with linear DNA in the thermotolerant yeast Kluyveromyces marxianus DMKU3-1042. Appl. Environ. Microbiol. 74, 7514–7521. https://doi.org/10.1128/AEM.01854-08.
Palmbos, P.L., Daley, J.M., Wilson, T.E., 2005. Mutations of the yku80 C terminus and Xrs2 FHA domain specifically block yeast nonhomologous end joining. Mol. Cell Biol. 25, 10782 https://doi.org/10.1128/MCB.25.24.10782-10790.2005.
Pley, H.W., Flaherty, K.M., McKay, D.B., 1994. Three-dimensional structure of a hammerhead ribozyme. Nat 3726501 372, 68–74. https://doi.org/10.1038/372068a0, 1994.
Ploessl, D., Zhao, Y., Cao, M., Ghosh, S., Lopez, C., Sayadi, M., Chudalayandi, S., Severin, A., Huang, L., Gustafson, M., Shao, Z., 2021. A repackaged CRISPR platform increases homology-directed repair for yeast engineering. Nat. Chem. Biol. 181 18, 38–46. https://doi.org/10.1038/s41589-021-00893-5, 2021.
Polotnianka, R.M., Li, J., Lustig, A.J., 1998. The yeast Ku heterodimer is essential for protection of the telomere against nucleolytic and recombinational activities. Curr. Biol. 8, 831–835. https://doi.org/10.1016/S0960-9822(98)70325-2.
Rajkumar, A.S., Morrissey, J.P., 2020. Rational engineering of Kluyveromyces marxianus to create a chassis for the production of aromatic products. Microb. Cell Factories 19, 1–19. https://doi.org/10.1186/S12934-020-01461-7/TABLES/3.
Rajkumar, A.S., Morrissey, J.P., 2022. Protocols for marker-free gene knock-out and knock-down in Kluyveromyces marxianus using CRISPR/Cas9. FEMS Yeast Res. 22, 67. https://doi.org/10.1093/FEMSYR/FOAB067.
Rajkumar, A.S., Varela, J.A., Juergens, H., Daran, J.-M.G., Morrissey, J.P., 2019. Biological parts for Kluyveromyces marxianus synthetic biology. Front. Bioeng. Biotechnol. 7, 97. https://doi.org/10.3389/fbioe.2019.00097.
Ryan, O.W., Cate, J.H.D., 2014. Multiplex engineering of industrial yeast genomes using CRISPRm. In: Methods in Enzymology. Academic Press Inc., pp. 473–489. https://doi.org/10.1016/B978-0-12-801185-0.00023-4
Ryan, O.W., Skerker, J.M., Maurer, M.J., Li, X., Tsai, J.C., Poddar, S., Lee, M.E., DeLoache, W., Dueber, J.E., Arkin, A.P., Cate, J.H.D., 2014. Selection of chromosomal DNA libraries using a multiplex CRISPR system. Elife 3. https://doi.org/10.7554/eLife.03703.
Schiffer, S., Rösch, S., Marchfelder, A., 2002. Assigning a function to a conserved group of proteins: the tRNA 3′-processing enzymes. EMBO J. 21, 2769–2777. https://doi.org/10.1093/EMBOJ/21.11.2769.
Schwartz, C., Shabbir-Hussain, M., Frogue, K., Blenner, M., Wheeldon, I., 2017. Standardized markerless gene integration for pathway engineering in yarrowia lipolytica. ACS Synth. Biol. 6, 402–409. https://doi.org/10.1021/ACSSYNBIO.6B00285/ASSET/IMAGES/LARGE/SB-2016-00285V_0004.JPEG.
Shanks, B.H., Keeling, P.L., 2017. Bioprivileged molecules: creating value from biomass. Green Chem. 19, 3177–3185. https://doi.org/10.1039/c7gc00296c.
Turowski, T.W., Tollervey, D., 2016. Transcription by RNA polymerase III: insights into mechanism and regulation. Biochem. Soc. Trans. 44, 1367–1375. https://doi.org/10.1042/BST20160062.
Urit, T., Stukert, A., Bley, T., Löser, C., 2012. Formation of ethyl acetate by Kluyveromyces marxianus on whey during aerobic batch cultivation at specific trace element limitation. Appl. Microbiol. Biotechnol. 96, 1313–1323. https://doi.org/10.1007/s00253-012-4107-z.
Verho, R., Londesborough, J., Penttilä, M., Richard, P., 2003. Engineering redox cofactor regeneration for improved pentose fermentation in Saccharomyces cerevisiae. Appl. Environ. Microbiol. 69, 5892–5897. https://doi.org/10.1128/AEM.69.10.5892-5897.2003.
Yang, C., Hu, S., Zhu, S., Wang, D., Gao, X., Hong, J., 2015. Characterizing yeast promoters used in Kluyveromyces marxianus. World J. Microbiol. Biotechnol. 31, 1641–1646. https://doi.org/10.1007/s11274-015-1899-x.

Yang, P., Zhu, X., Zheng, Z., Mu, D., Jiang, S., Luo, S., Wu, Y., Du, M., 2018. Cell regeneration and cyclic catalysis of engineered Kluyveromyces marxianus of a d-psicose-3-epimerase gene from Agrobacterium tumefaciens for d-allulose production. World J. Microbiol. Biotechnol. 34, 1–7. https://doi.org/10.1007/S11274-018-2451-6/TABLES/1.

Zhang, B., Ren, L., Wang, H., Xu, D., Zeng, X., Li, F., 2020a. Glycerol uptake and synthesis systems contribute to the osmotic tolerance of Kluyveromyces marxianus. Enzym. Microb. Technol. 140, 109641 https://doi.org/10.1016/J.ENZMICTEC.2020.109641.

Zhang, B., Ren, L., Zeng, S., Zhang, S., Xu, D., Zeng, X., Li, F., 2020b. Functional analysis of PGI1 and ZWF1 in thermotolerant yeast Kluyveromyces marxianus. Appl. Microbiol. Biotechnol. 104, 7991–8006. https://doi.org/10.1007/S00253-020-10808-4/FIGURES/8.

Zhang, J., Zhang, B., Wang, D., Gao, X., Sun, L., Hong, J., 2015. Rapid ethanol production at elevated temperatures by engineered thermotolerant Kluyveromyces marxianus via the NADP(H)-preferring xylose reductase-xylitol dehydrogenase pathway. Metab. Eng. 31, 140–152. https://doi.org/10.1016/J.YMBEN.2015.07.008.